3rd URSI AT-AP-RASC, Gran Canaria, 29 May – 3 June 2022

Estimation of polarization effects on sky visibilities for FARSIDE

Nivedita Mahesh*(1), Bharat Gehlot(1), Judd Bowman(1), and Daniel Jacobs(1)
(1) School of Earth and Space Exploration, Arizona State University, Tempe, Arizona, USA

Abstract

The Farside Array for Radio Science Investigations of the Dark ages and Exoplanets (FARSIDE) is a NASA funded probe-class mission concept to place a radio array (100 kHz - 40 MHz) on the far side of the Moon. The nominal array design consists of 128 non co-spatial orthogonal pairs of antenna and receiver nodes distributed over a 10 km $\times$ 10 km area in a four arm spiral configuration. In this work we quantify the polarization leakages, due to dipole offsets, in terms of the stokes I, Q, U, and V beams as a function of sky position. We find that the offset leads to additional mixing and leakages of all Stokes components of the sky into the U and V polarizations of the instrument. We develop a custom interferometer pipeline for FARSIDE incorporating the co-spatial and non co-spatial Stokes beams and the *uv*-coverage of the array. We calculate the sky visibilities and produce the dirty images of point sources of the GLEAM catalog. Using the results, we estimate the effects of spatially non co-located antennas on the imaging performance of the array.

1 Introduction

Low-frequency, sub-MHz, radio astronomy can reliably be performed only from space. Because at frequencies below 40 MHz, there is heavy contamination on the Earth's surface by anthropogenic radio frequency interference (RFI), corruption by the ionosphere via its absorption and emission that intensifies below $\approx$ 10 MHz [1], and refraction by solar emissions and solar wind [2]. There is important science to be observed at these low frequencies including search for radio signatures of coronal mass ejections and energetic particle events, detection of the magnetospheres for the nearest candidate habitable exoplanets, and understanding of the unexplored epoch of the universe's formation - The Dark Ages. In line with this, FARSIDE (Farside Array for Radio Science Investigations of the Dark ages and Exoplanets) is a concept for a probe mission to place a low-frequency radio interferometric array on the lunar farside. FARSIDE will take advantage of NASA's Artemis program investments, which are expected to reach sufficient maturity by the mid-2020s to support a mission in the 2025–2035 time frame. The notional architecture of the probe mission design study consists of 128 dual polarization antennas spanning a 10 km area. Rovers will deploy the array and tether it to a base station for central processing, power, and data transmission to the Lunar Gateway [3].

FARSIDE will prove to be a powerful instrument for two of the most profound questions in astrophysics today: radio emission detection from exoplanets to complement the search for habitability and exploration of the Dark Ages through Hydrogen cosmology. In any interferometer, instrumental effects cause inter-mixing of the intrinsic source polarizations. In the case of FARSIDE, there is an offset between the dipoles of each antenna node in the array that causes additional mode mixing and increases the polarization leakage. To quantify this effect and maximize its performance for the desired science cases, we perform a study on its polarization imaging performance while taking advantage of its deployment strategy.

2 FARSIDE design and nominal array layout

The currently planned array layout of the FARSIDE instrument is a four arm spiral with 32 pairs of dipoles on each arm that are tethered to the central base station as shown in Fig. 1. Four two-wheeled tethered rovers would be teleoperated to deploy the nodes on the four-arm spiral that remain connected to the lander by their individual tethers, providing communication, data relay, and power during deployment as well as for operations [3]. To enable the desired science cases, the antenna and the array are designed to operate from 100 kHz to 30 MHz. The chosen length of the dipole is 100 m for the entire bandwidth of operation. These dipoles cannot be deployed using stacers, so for ease of deployment, the final design is to embed the dipoles sequentially in the tethers that connect the individual nodes. In this scenario, the rover will deploy the tether with 90° bends along its path at each antenna location to ensure that the two embedded dipoles are aligned to orthogonal polarizations thus leading to an offset between the phase centers of the dipoles (Fig. 2). This design provides for dual polarization measurements, circular polarization data that can help confirm exoplanet radio emissions and reduce integration time by a factor of 2. For both the key science cases of FARSIDE we need high fidelity polarization data. For the exoplanet studies we need circular polarization information to separate the planet's signal from that of the star's in the acquired sky data. To detect the faint high redshift 21-cm signal we need the Stokes V information for precise estimation of the instrumental noise.

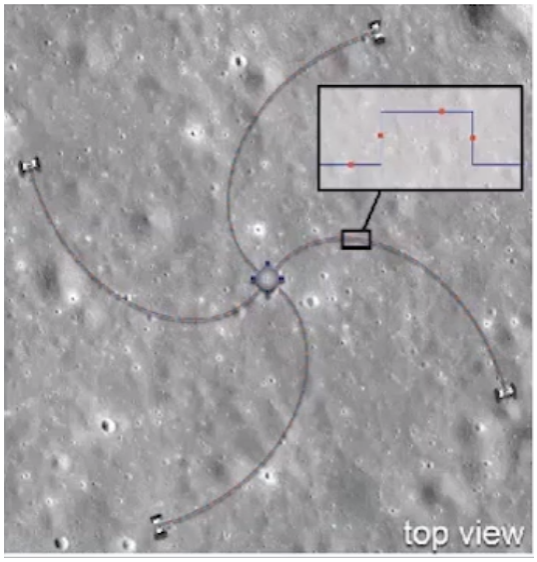

Figure 1. An artist's rendering of the four arm spiral configuration of the FARSIDE array on the lunar surface. At the centre of the array is the base station with the communication antenna, fuel tank, central processing unit with correlators and the main power supply. Each of the four spiral arms, will have 32 antenna nodes consisting of two dipoles and a receiver. Also shown are the four two-wheeled rovers that will deploy the tethers containing the antenna nodes. The inset image shows the path taken by the rover to lay out the embedded dipole antennas with the 90 deg bend at each antenna node. The phase centers of the dipoles are indicated by the red dots.

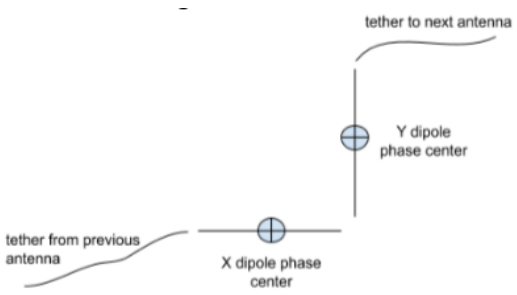

Figure 2. A sketch detailing the deployment configuration for a single antenna node of FARSIDE. The tether from previous antenna node leads upto one of the dipoles (X-dipole), then the rover turns 90^o lays out the orthogonal dipole (y-dipole) and carries the tether over to the location of the next node.

3 Understanding the effects of spatially non colocated antenna pairs

We use a simple two element interferometer to understand the effect of offsets between polarizations of the same antenna pair. In the top panel of Fig. 3, the X and Y dipoles of each antenna node are spatially co-located. To coherently look at the signal arriving from the source at the top right we would just need to add a single delay of τ to both the orthogonal dipoles of antenna 2 to compensate for the timing of the signal arriving at antenna 1. This is implemented in most current and next generation radio interferometers like MWA, HERA, LOFAR, GMRT, VLA, and WSRT, to name a few. In the bottom panel of Fig. 3, we introduce an offset between the two polarizations of each antenna. This is a simplified schematic showing delay in a single dimension. However, 2D arrays require delay corrections in two dimensions. This results in an additional delay of τ_o between the x and y dipole of each antenna. And to coherently add the signal from the same source at all dipoles we will need a delay of $\tau_o + \tau$ at Y_2, τ at x_2, and τ_o at x_1. Such polarization offsets are also seen in radio arrays like 21CMA as well as feeds of ASKAP and APERTIF.

We investigate the effects on imaging performance of the FARSIDE due to the offset between the dipole pairs in each antenna node. To do this, we simulate all the antenna positions (phase centers) of the spiral configuration. The notional design is that the X and Y dipoles will have an offset of 50m in the X and Y directions. This is the minimum offset required to fit 2 dipoles, each with a half arm length of 50m, sequentially. For all the analyses in this paper we assume the ideal offsets between the X and Y polarization to be $\Delta x = 50m$ and $\Delta y = 50m$.

The offset causes the sets of XY and YX baselines to fill different regions in visibility space compared to corresponding XX and YY polarizations. The perturbed array (with offset) will have the XY/YX pairs form baselines that span a wider range of *uv*-values compared to the XX/YY baselines and hence fill in the *uv*-space better than the latter. This in turn results in a better PSF for the XY baselines as shown in the bottom of Fig. 3 where the PSF of the XY baseline has 3×lower values at points 15 deg and beyond from the zenith.

4 Estimating the effects of polarisation leakage on the beam

We simulated a pair of 100 m orthogonal dipoles placed directly on the regolith in two cases, one with the phase centers co-located and the other with a diagonal offset of $50\sqrt{2}$ m between the phase centers. We set the dielectric properties of the regolith using values from the Lunar source book which reported the relative permittivity, $\varepsilon_r = 2$ and conductivity, $\rho = 10^{-3}\ S/m$. The electric beam patterns obtained from the FEKO Electromagnetic simulations

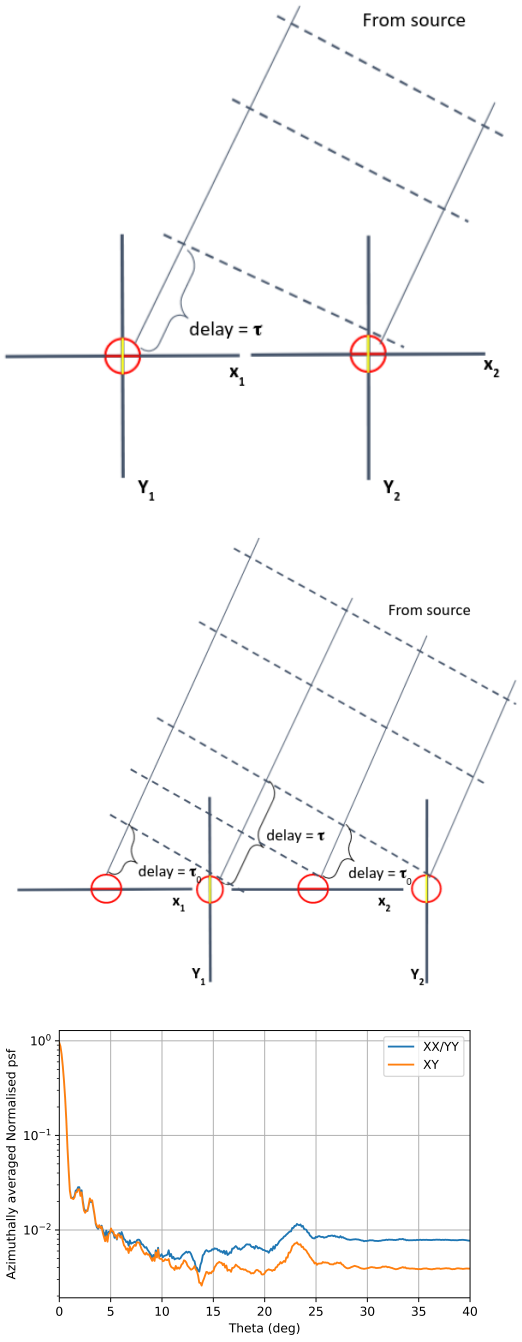

Figure 3. [top middle]A schematic highlighting the difference between the spatially co-located and non co-located dipoles in a 2 element interferometer. The offset between the phase centers results in an additional delay(τ_o) between the X and Y combinations of each antenna pair. Additional corrections are needed when cross correlating data from different antennas. [Bottom] Azimuthally averaged Point Spread function versus elevation angle for the two cases of the FARSIDE spiral arm layout: a.) without offset and b.) with offset between the orthogonal polarization dipoles.

are used to calculate the direction-dependent Jones matrix for an antenna node i, in the FARSIDE array, as follows:

$$J_{\mathrm{beam},i}(\hat{s},\nu) = \begin{bmatrix} E^x_\theta(\hat{s},\nu) & E^x_\phi(\hat{s},\nu) \\ E^y_\theta(\hat{s},\nu) & E^y_\phi(\hat{s},\nu) \end{bmatrix} \quad (1)$$

Unless J_{beam} is both diagonal and has, at any given point on the sphere, equal diagonal elements, there will be mixing or "leaking" of different Stokes parameters together into each element of the visibility vector in a direction dependent way [5].

The direction dependent Stokes leakage in the visibilities can be quantified using the Muller matrices that map the sky Stokes parameters to the pseudo-Stokes formed using the visibilities given as follows:

$$\mathscr{V}^n_{ij}(\nu) = \int (M_{n0}I + M_{n1}Q + M_{n2}U + M_{n3}V) exp(-2\pi i \nu b.\hat{s}/c) d\Omega \quad (2)$$

where n goes from 0 to 3 and corresponds to pseudo-Stokes I, Q, U and V.

We calculate the Muller matrices from the visibilities that are given by the sky coherence and the antenna beam. This procedure is adapted from [4].

$$\begin{bmatrix} E_{\mathrm{XX}} & E_{\mathrm{XY}} \\ E_{\mathrm{YX}} & E_{\mathrm{YY}} \end{bmatrix} = J \times \mathscr{C} \times J^H$$

where:

$$\text{Sky coherence}, \mathscr{C} = \begin{bmatrix} I+Q & U-iV \\ U+iV & I-Q \end{bmatrix}$$

Examples of M_{ij} at 2 MHz ($\approx$ central frequency in the band of interest) for the non offset (only the effect of the beam) case are shown in Figure 4, projected in the theta/phi basis. All of the dynamic ranges are normalized to the peak of M_{00}, which is 1 at zenith. For an ideal instrument, with no mode mixing, the off diagonal Muller matrices would be zero. The first row corresponds to the Sky Stokes I coupling into the instrument's all 4 stokes components. Similarly, the second, third and fourth columns capture the Sky's stokes components into all the 4 pseudo-stokes visibilities of the instrument. For the exoplanet science case, we are concerned about the Muller matrices M_{30}, M_{31} and M_{32}; leakage of the Sky components into the measured Stokes V. In the case of no offset it is at least 2 orders magnitude lower.

We calculate the similar Muller matrix for the non-colocated dipoles as shown in Fig. 5. The same procedure is followed, but an additional Jones matrix is added to account for the differential delay due to the offset of the dipole phase centers:

$$J_{\mathrm{offset}} = \begin{bmatrix} 1 & 0 \\ 0 & e^{i\Delta\phi} \end{bmatrix}$$

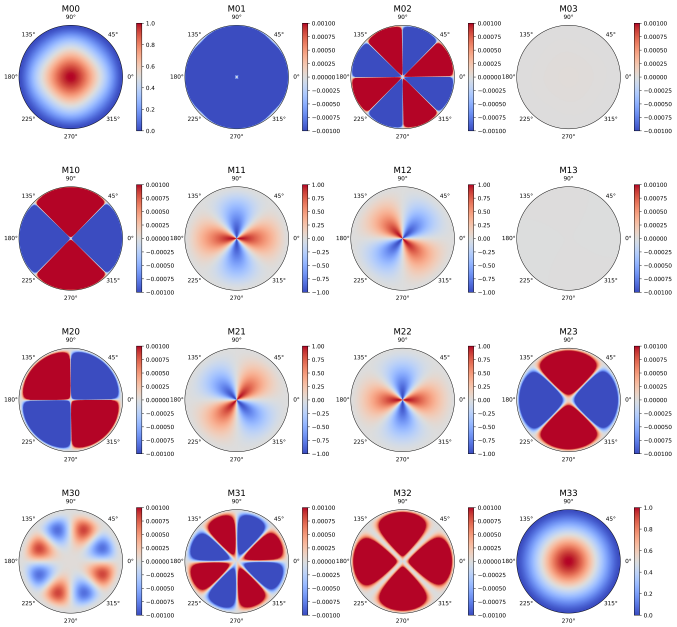

Figure 4. Simulations of the dipole beam and the offset on the direction dependent Mueller matrix at 2 MHz projected into the RA, Dec basis. Color scales for frequencies are relative to the peak of M_{00} (which itself is normalized to 1 at zenith). For a key to these matrices, see Equation 9.

The visibility matrix is also redefined as:

$$\begin{bmatrix} E_{XX} & E_{XY} \\ E_{YX} & E_{YY} \end{bmatrix} = (J_{\text{offset}} \times J_{\text{beam}}) \times \mathscr{C} \times (J_{\text{offset}} \times J_{\text{beam}})^H$$

Comparing the two plots (Fig. 4 5) there is a significant impact due to the dipole offset on the leakage of the Stokes U & V (the bottom two row of the no offset case with the two rows of the offset). The simulated Stokes leakage is shown just for one frequency (2 MHz). However, the Stokes leakage varies with frequency and has been found to increase with frequency.

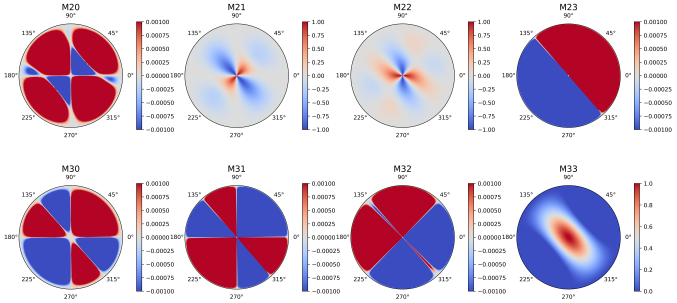

Figure 5. Simulations of the dipole beam direction dependent Mueller matrix for Stokes U V at 2 MHz projected into the RA, Dec basis. Color scales for frequencies are relative to the peak of M_{00} (which itself is normalized to 1 at zenith). For a key to these matrices, see Equation 9.

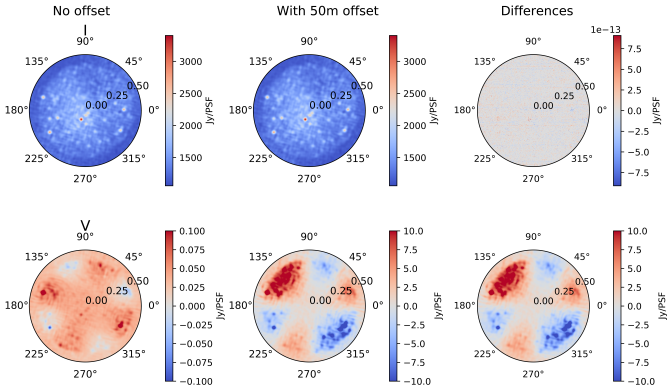

Figure 6. Constructed Stokes I [top] V [bottom] images of the GLEAM source catalog processed through the beam and uv-coverage of FARSIDE. The images are produced for two cases: [left] the beams of the orthogonal dipoles with the same phase center and, [right] beams of the orthogonal dipoles with an offset of 50m between the phase centers. The custom pipeline (at the moment) does not take into account wide field effects so we have clipped sources >30 deg from zenith.

5 Estimating the effects of polarisation leakage on model sky

We further extend our analysis to estimate the effects on a model sky. For our model sky we use the GLEAM point source catalogue. We develop a custom interferometer pipeline that takes the fourier transform of the different polarization beams (both offset and non-offset beams) and *uv*-coverage of the FARSIDE array and then calculate the sky visibilities to produce dirty images of the sky. Preliminary analysis shows that offset between the dipoles leads to considerable Stokes V leakage. Thus calibrating out the effects of the offset is essential for the desired science cases.

6 Conclusion

FARSIDE layout has a spatial offset between the orthogonal dipoles for easy deployment. We have performed a detailed analysis to access the performance of the array. We have studied the effects of the non colocated dipoles on the *uv*-coverage, PSF and Stokes leakage. We have developed a pipeline to study the beam and offset effects on the obtained polarized images. We are currently investigating methods to calibrate U and V.

7 Acknowledgements

This work is directly supported by the NASA Solar System Exploration Research Virtual Institute cooperative agreement number 80ARC017M0006. N.M. was supported by the Future Investigators in NASA Earth and Space Science and Technology (FINESST) cooperative agreement 80NSSC19K1413.

References

[1] Rogers, A. E. E., Bowman, J. D., Vierinen, J., Monsalve, R. and Mozdzen, T., "Radiometric measurements of electron temperature and opacity of ionospheric perturbations.", Radio Science, **50**, 2015, pp. 130– 137. doi: 10.1002/2014RS005599.

[2] Liu, L., Chen, Y., Le, H., Kurkin, V. I., Polekh, N. M., and Lee, C.-C. (2011), "The ionosphere under extremely prolonged low solar activity", *Journal of Geophysical Research*, **116**, 2011, A04320, doi:10.1029/2010JA016296.

[3] Burns, J., "Global 21-cm Cosmology from the Farside of the Moon", *arXiv e-prints*, 2021.

[4] Kohn, S. A., "The HERA-19 Commissioning Array: Direction-dependent Effects", *The Astrophysical Journal*, vol. 882, no. 1, 2019. doi:10.3847/1538-4357/ab2f72.

[5] Smirnov, O. M., "Revisiting the radio interferometer measurement equation. I. A full-sky Jones formalism", *Astronomy and Astrophysics*, vol. 527, 2011. doi:10.1051/0004-6361/201016082.